Relation between mainshock rupture process and Omori's law for aftershock moment release rate

by Yan Y. Kagan and Heidi Houston

Dept. Earth & Space Sciences, UCLA, ykagan@ ucla.edu, 310-206-5611; fax 310-825-2779, http://scec.ess.ucla.edu/ykagan.html

Abstract

We compare the source time functions (moment release rates) of three large California mainshocks with the seismic moment release rates during their aftershock sequences. Aftershock moment release rates, computed by summing aftershock moments in time intervals, follow Omori's law from minutes to months after the mainshock; furthermore, in contrast to the previously-observed saturation in numbers of aftershocks shortly after the mainshock rupture, no such saturation is seen in the aftershock moment release rates, which are dominated by the largest aftershocks. We argue that the observed saturation in aftershock numbers described by the "time offset" parameter c in Omori's law is likely an artifact due to the under-reporting of small aftershocks, which is related to the difficulty of detecting large numbers of small aftershocks in the mainshock coda. We further propose that it is more natural for c to be negative (i.e., singularity follows the onset of mainshock rupture) than positive (singularity precedes onset of rupture).

To make a more general comparison of mainshock rupture process and aftershock moment rates, we then scale mainshock time functions to equalize the effects of the varied seismic moments. For the three California mainshocks, we compare the scaled time functions with similarly-scaled aftershock moment rates. Finally, we compare global averages of scaled time functions of many shallow events to the average scaled aftershock moment release rate for six California mainshocks. In each of these comparisons, the extrapolation of the aftershock moment rates according to Omori's law back in time toward the mainshock rupture indicates that the temporal intensity of the aftershock moment release is about 1.5 orders of magnitude less than the maximum reached by the mainshock rupture. This may be due to the differing amplitudes and relative importance of static and dynamic stresses in aftershock initiation compared to mainshock rupture propagation.

See manuscript at http://scec.ess.ucla.edu/~ykagan/heidi_index.html

How does moment release during a mainshock relate to aftershock decay?

A. Omori's (1894) law describes the decay of aftershock activity with time:

$$n(t) = \frac{K}{t+c},$$

where n(t) is aftershock frequency measured over a certain interval of time.

Utsu (1961) proposed a modified Omori's law

$$n(t) = \frac{K}{(t+c)^p},$$

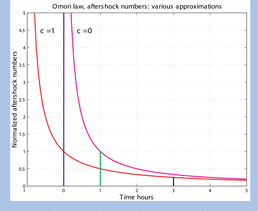

Many empirical studies have found a positive value of c of order 12 hours. A positive c > 0 in Omori's law means that the singularity in aftershock rate occurs at negative time (t<0), i.e., before the mainshock. The plots show Omori Laws with c = 1 and c= 0 in linear scale (above) and log-log scale (below). We propose that the positive empirical value for c is mostly due to the under-reporting of small aftershocks immediately following a mainshcok (Kagan, 2004).

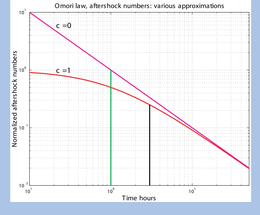

B. The threshold for aftershock completeness decreases with time following the mainshock

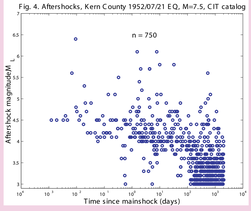

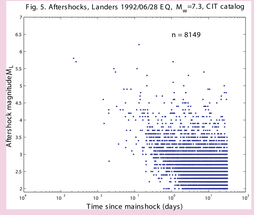

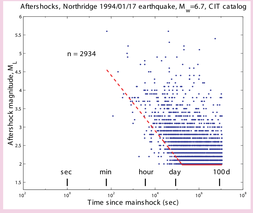

Time-magnitude distribution of aftershock sequences of several California mainshocks: Kern County, Landers, and Northridge, using data from the Caltech catalog. The aftershock sequence of the 1994 M=6.7 Northridge, California is shown on the right. For Northridge the window is latitude 34.0-34.5 N, longitude 118.35-118.80 W; the time interval is 128 days after the mainshock. With increasing time after the mainshocks, the catalog is complete to a lower magnitude threshold. Kagan (2004) concluded that aftershocks are underreported following a large mainshock due to factors including the mainshock coda, the overlapping of aftershocks, and workforce constraints. These effects decrease with time, leading to the decrease in the completeness threshhold. The red dashed line shows an estimate of the completeness threshold (see also Helmstetter, Kagan and Jackson, SCEC poster, 2004), which can be used to correct aftershock frequency and moment release rate for missing aftershocks.

C. Comparisons of moment release rates during mainshocks (i.e., source time functions) and aftershock sequences

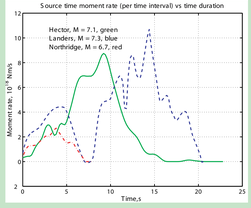

Source-time functions (i.e., moment release rates) for three California earthquakes: 1992 M 7.3 Landers (dashed blue line), 1994 M 6.7 Northridge (dash-dotted red line), and 1999 M 7.1 Hector Mine (solid green line).

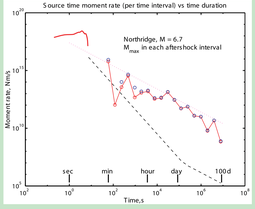

Source-time function for 1994 M 6.7 Northridge, California earthquake compared to moment release (red circles) of its immediate aftershocks, averaged over logarithmic time intervals. Blue circles show aftershock moment release corrected for under-reported small aftershocks (Kagan, 2002), using the aftershock moment threshold (black dashed line) divided by the duration of the corresponding time interval to yield quantities comparable to the moment rate. The dotted line shows a power-law approximation for aftershock moment release rates, analogous to Omori's law.

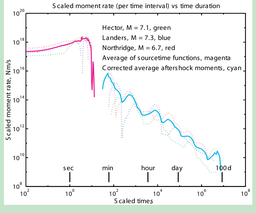

Scaled source-time functions for three California earthquakes: 1992 M7.3 Landers (blue line), 1994 M6.7 Northridge (red line), and 1999 M7.1 Hector Mine (green line) and moment release of their aftershock sequences, corrected for missing small aftershocks and averaged over logarithmic time intervals. Scaling is performed to normalize source time functions and aftershock moment rates to account for effect of differing mainshock magnitudes (Houston, 2001). Averages of scaled source-time functions and aftershock sequences shown by solid lines.

Source time functions and aftershock moment release rates can be normalized to account for the effect of varying mainshock moments. Such scaling allows the averaging of data for mainshocks of different moments. The time axis is scaled by the inverse cube-root of moment, while the amplitudes are scaled by the inverse two-thirds power of moment (Houston, 2001). Here we scale all mainshocks and aftershock sequences to a magnitude 6.67 event.

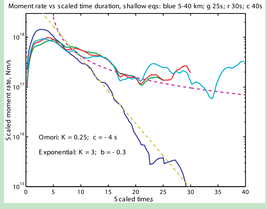

Average scaled seismic moment source-time functions for 143 shallow (5-40 km) global earthquakes (Houston, 2001), and their approximation by an exponential function (yellow) and a power-law (Omori) distribution (magenta). For the latter approximation we use c = -4 s, which is close to the rupture time of m=6.67 earthquake. Blue curve shows the average of scaled time functions truncated at the inferred end of rupture. Green, red, and cyan curves show averages of subsets of source-time functions comprising those non-truncated time functions for which the s.t.f inversion result was available for at least 25, 30, and 40 scaled seconds (i.e., including a sufficient interval after the apparent end of mainshock rupture). For the non-truncated time functions, moment release at the end of mainshock rupture seems to decay as 1/t similar to Omori's law.

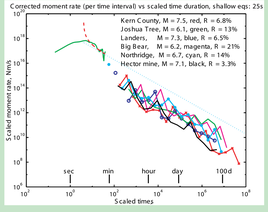

Average scaled source-time function for shallow global earthquakes (non-truncated time functions, see left) compared to scaled aftershock moment release rates for six California aftershock sequences. Both types of moment rates were scaled to m=6.67 earthquake. Two Omori law approximations to the source time functions are shown with c = -4 s, and with c = 0. The California aftershock sequences were corrected for missing small aftershocks (Kagan, 2002). The coefficient R in the figure is the percent of total seismic moment released by immediate aftershocks compared to the mainshock scalar moment. The activity level in the aftershock sequences extrapolates to about 30 times less than the maximum rate in the average scaled global time function.

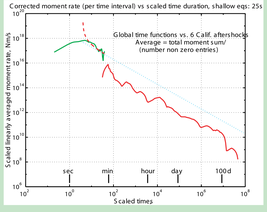

Average scaled source-time function for global shallow earthquakes with non-truncated time functions (green line) compared to corrected scaled average for six California aftershock sequences (red line). Approximations of average time function by power-law (Omori) distributions (dashed and dotted lines) are also shown. As before, two Omori law approximations are given with c = -4 s, and with c = 0 s. The average aftershock rates fall about 8 orders of magnitude over about 200 days. Extrapolating back in time according to Omori's law yields a level of aftershock activity about 1.5 orders of magnitude less than the maximum mainshock moment rate.

Selected References:

Houston, H., 2001.
Influence of depth, focal mechanism,and tectonic setting on the shape and duration of earthquake source time functions, J. Geophys. Res., 106, 11,137-11,150.

Kagan, Y. Y., 2002.
Seismic moment distribution revisited: II. Moment conservation principle, Geophys. J. Int., 149, 731-754.

Kagan, Y. Y., 2004.
Short-term properties of earthquake catalogs and models of earthquake source, Bull. Seism. Soc. Am., 94(4),1207-1228.

Omori, F., 1894.
On the after-shocks of earthquakes, J. College Sci., Imp. Univ. Tokyo, 7, 111-200.

Utsu, T., 1961.
A statistical study on the occurrence of aftershocks, Geoph. Magazine, 30, 521-605.

Conclusions

1. Moment release rates during mainshocks (i.e., source time functions) are compared with moment release rates during aftershock sequences.

2. From minutes to months following a mainshock, the moment release rate of the aftershock sequence follows a power-law decay similar to the familiar Omori law for aftershock frequency. We note inconsistencies in the standard Omori formula, and propose that the positive value for c found empirically by many studies is mainly due to the underreporting of small aftershocks.

3. We made various comparisons of individual California earthquakes and global averages of shallow earthquakes with individual aftershock sequences and an average California aftershock sequence. Before averaging, the time functions and moment release rates of aftershocks were scaled to normalize for the effect of varying mainshock seismic moments.

4. In all the comparisons the extrapolation of the aftershock moment rates back in time following Omori's law yields a rate about 30 times smaller than the maximum moment rate of the mainshock. This difference likely reflects the key role of dynamic wave/stress propagation that drives rupture.